

Article

Evaluation of Coastal Protection Strategies at Costa da Caparica (Portugal): Nourishments and Structural Interventions

Francisco Sancho 

Laboratório Nacional de Engenharia Civil, 1700-066 Lisboa, Portugal; fsancho@lnec.pt; Tel.: +351-218443664

Abstract: Costa da Caparica beach, in Portugal, has suffered from chronic erosion for the last 50 years, a phenomenon that has been countered by various management interventions. This study aims at comparing sixteen possible interventions, thus identifying the most effective one(s) in terms of reducing beach erosion or even promoting beach accretion. This exercise is achieved using a one-line shoreline evolution model, calibrated with in situ field data, forced by local wave conditions. The target management period is 25 years. In the calibration phase, it is found that the annual mean alongshore net sediment transport along the 24 km sandy coast is variable in direction and magnitude, but it is mostly smaller than $\pm 50 \times 10^3 \text{ m}^3/\text{year}$. This net transport results from the imbalance of northward/southward-directed bulk transports of circa tenfold-larger magnitudes. This affects the overall sediment balance at the urban beaches, as well as the effectiveness of the intervention strategies. The results show that the present management strategy is effective in holding the shoreline position, although deploying the same nourishment volume but over a shorter area could lead to better results. The best solutions, which are capable of promoting beach accretion, implicate the lengthening of the terminal groin at the northern extremity of the beach. The results from this study can support decision makers in identifying the most appropriate management action, not just locally but also at other coastal regions where similar problems persist and the same methodology could be applied.

Keywords: one-line model; coastal erosion; sediment transport; coastal management; groin field



Citation: Sancho, F. Evaluation of Coastal Protection Strategies at Costa da Caparica (Portugal): Nourishments and Structural Interventions. *J. Mar. Sci. Eng.* **2023**, *11*, 1159. <https://doi.org/10.3390/jmse11061159>

Academic Editor: Yuanzhi Zhang

Received: 17 April 2023

Revised: 22 May 2023

Accepted: 26 May 2023

Published: 31 May 2023



Copyright: © 2023 by the author. Licensee MDPI, Basel, Switzerland. This article is an open access article distributed under the terms and conditions of the Creative Commons Attribution (CC BY) license (<https://creativecommons.org/licenses/by/4.0/>).

1. Introduction

Over the last century, coastal management has been addressed and confronted with varying strategies and responses, with many successful and failure stories from which we can learn and achieve a more efficient integration of the socio-economic systems with natural coastal ecosystems [1]. Sandy beaches can enter into sediment unbalance and suffer from erosion problems, affecting the socio-economic value of the area and, conceivably, endangering people and goods [2–4].

Fifty years ago, coastal management responses were typically reactive, based mainly on structural engineering measures that aimed to provide protection against flooding, safety and space for beach recreation and, occasionally, natural conservation. Currently, preventive strategies with risk-based analysis frameworks are often employed, which combine structural and non-structural measures such as hard and soft protective measures, land use planning and ecosystems services, early warning/evacuation strategies, education and insurance schemes [5–7].

While the protection of coasts is becoming a global priority, there is no consensus on the actual meaning of “coastal protection” [7]. To some, this may mean resistance management, to halt coastal erosion and protect property; to others, it means pro-adaptive management, allowing coastal ecosystems to function naturally [6] and, in many cases, retreat. The outcomes of these different perceptions are contrasting. This paper analyses different management policies aligned with the first option—halting coastal erosion and protecting property.

At Costa da Caparica town (near Lisbon, Portugal, see location in Figure 1), human encroachment is responsible for degradation and loss of coastal ecosystems over recent decades [8]. The beach suffers from chronic erosion [9,10] and has been subject to several coastal protection measures since the early 1970s, involving both hard and soft protection measures. In general, the hard measures built to prevent erosion (such as seawalls or groins) further limited the coast from adjusting to the changing conditions. The naturally existing foredunes could no longer translate upwards and landwards as the sea level rose and the coast eroded, because the infrastructure occupied the required space. Consequently, the resilience and resistance of the coast and its ecosystem services are being lost, diminished, or put at risk. In addition, this coastal town is exposed to rising sea levels, erosion, flooding, tsunamis and extreme hydro-meteorological events (e.g., [11]). Problems remain; in particular, the narrow beach width is unable to withstand the beach-use summer crowds and economic losses due to coastal overtopping (e.g., [12]); hence, future actions and strategies need to be evaluated.



Figure 1. Study area with place names, reference or baseline (deep orange) and 8, 16 and 30 m isobaths. (Adapted from geomar.hidrografico.pt, accessed on 20 May 2023, using ESRI World Imagery).

The use of numerical models for predicting shoreline behaviour in the future is a widely used practice (e.g., [3]). Shoreline evolution models are simple but robust enough, when properly calibrated, to help analyse different coastal management options (e.g., [13,14]) or changes in the forcing mechanism (e.g., [15]). A recent review highlighting the capabilities and restrictions of one-line models is given by Chataigner et al. [16].

This paper aims at comparing different intervention strategies at Costa da Caparica beaches, comprising soft- and hard-engineering solutions (as detailed in Section 3.2.4), using a one-line shoreline evolution model. This provides a unique framework to assess possible coastal management interventions.

2. Study Area

The study area comprises the Atlantic ocean sandy beach immediately south of Lisbon (Portugal), which extends southward from *Cova do Vapor* to *Praia da Pipa* (Figure 1). This coastal stretch includes: (i) a northern sector—Costa da Caparica beaches—strongly intervened by artificial structures, protecting the town with the same name; (ii) a low-lying beach–dune system extending southwards from Costa da Caparica until *Fonte da Telha*; (iii) a sandy beach backed by soft (sandstone/clay stone) coastal cliffs; and (iv) the intermittently opened coastal lagoon *Lagoa de Albufeira*. South of the sandy beach, the littoral arch is completed by limestone cliffs until *Cape Espichel* (to the south of the region shown in Figure 1).

At the northern extreme, *Cova do Vapor* faces the Tagus river mouth, a tide-dominated estuary, with complex morphological interactions and evolution [17], which also affects the Costa da Caparica beach sediment transport fluxes and stability. Along the 5 km stretch to the south of *Cova do Vapor*, the coastline presents an alluvial plain with strong anthropogenic occupation [17].

Costa da Caparica beach (Figures 2 and 3) is an urban beach, with buildings constructed over foredunes, and part of the approximately 24 km low-elevation sandy beach sector, with a predominantly NNW–SSE orientation. Coastal defence works in the area include two groins (EV1 and EV2) at *Cova do Vapor*, delimiting the Tagus river entrance, and seven groins (EC1 to EC7) and one ~2.9 km long rock armour revetment at Costa da Caparica beaches (Figure 3). Figure 2 illustrates two photographs, one showing the beach to the north of Caparica, named *Praia de São João da Caparica*, and the other an urban beach, in front of the town, confined by groynes and a coastal revetment.



Figure 2. Images of Costa da Caparica beaches: *Praia de São João da Caparica* (left), and central urban beach, confined by groynes and an inland revetment (right).

According to Lira et al. [18], between 1958 and 2010, the entire sector presented a relative stability, with minor erosive tendency of -0.04 ± 0.03 m/year. However, the northern sector of Costa da Caparica exhibited a spatial maximum coastal retreat of -4.57 ± 0.2 m/year, whereas the sandy beaches at the south of the coastal arch presented accretion with a maximum of 1.20 ± 0.2 m/year. These data agree with the findings of Silva et al. [11], who report mean retreat rates of -3.09 ± 1.12 m/year at *São João da Caparica* beach (between groins EC7 and EV1; see location in Figure 3) and -1.69 ± 1.94 m/year at the urban beaches of Costa da Caparica, from the analysis of shoreline evolution data from 1958 to 2013. Accordingly, Pinto et al. [19] reported erosion over 200 m in the past 60 years at Costa da Caparica.

In order to counteract this erosive tendency, between the late 1950s and early 1970s, a groin field and a seawall/revetment were built in order to stabilize the shoreline and, tentatively, increase the beach width. However, coastline stabilization was not enough to reduce beach erosion and protect inland infrastructures. Between 1995 and 2003, several erosive episodes were reported north of Costa da Caparica, followed by emergency repair works (such as dune reinforcement) between 2003 and 2004, and strengthening and reconfigura-

tion of the groin field and seawall from 2004 to 2006 [9,20]. Afterwards, according to the designed coastal management master plan [21], an extensive beach nourishment program was carried on by Portuguese coastal authorities between 2007 and 2019, comprising the placement of 4.5 million m³ of sand (in five phases) in the sub-aerial beach, along the 3.8 km northern shoreline. Sand sources came from regular maintenance dredging performed by the Lisbon Port Authority (APL) in the outer Tagus estuary navigation channel (located 7 to 9 km from the project site) [19].



Figure 3. Groin's identification at Costa da Caparica beach.

According to Silva et al. [11], from the analysis of a 35-year long hindcast record, the area is frequently affected by moderate wave conditions with significant wave heights lower than 2 m with a dominant NNW–SSE direction. Raposeiro et al. [22] and Garzon et al. [23] indicate that the averaged significant wave height at the entrance of the Tagus river (at an approximate depth of 24 m Chart Datum, C.D.) is 1.22 m and 1.19 m, respectively. The averaged mean wave direction and mean wave period are 280° and 5.7 s, respectively. Sancho et al. [24] presented the wave climate spatial variation along the coastal arch, where an increase in the mean wave direction from north to south (from approx. 230° to 285°) is noticeable, as well as an increase in the mean significant wave height from half the coastal arch until the southern end. Dodet [25] reveals a high seasonal variability in the wave climate in front of *Lagoa de Albufeira*, with a maximum mean value in January (1.6 m) and a minimum mean value in August (0.8 m). Similarly, those results also exhibit a large seasonal variability in the significant wave height standard deviation, with larger values during the winter period (up to 0.4 m) than during the summer period (up to 0.1 m).

Regards to astronomical sea level variation, the study area is affected by semi-diurnal tides, with a mean tidal range of 2.20 m recorded in *Cascais* (west of Lisbon) tide gauge [11].

In front of Costa da Caparica beaches, the residual tidal currents intensities are much lower than at the river mouth, of the order of 0.2 m/s, directed northward [26].

The magnitude and net direction of the longshore sediment transport at Costa da Caparica and the coastal arch *Caparica-Espichel* has been subject to debate [24]. While some authors (e.g., [27]) advocate that the net alongshore yearly mean sediment transport is directed south to north over the entire sector, other results have pointed out that the net transport has the opposite orientation, for example, in front of *Lagoa de Albufeira* [25]. Recent results by Sancho [28] sustain that the net transport is indeed northward oriented in the northern sector of the coastal arch (in the first 5 km south of *Cova do Vapor*), and then the net direction changes southward, with increasing magnitudes towards the south. At Costa da Caparica beaches, the net transport is of the order of 50,000 m³/year [28], resulting from the (in)balance of larger bulk transports, in either direction. At the groin-confined urban beaches, the bulk transports are lower than those at non-confined beaches, due to sand retention at the structures. It is worth noticing that, at *São João da Caparica*, Sancho [28] identified an inter-annual variability in the net alongshore sediment transport rates and direction, despite the long-term averaged value being northward directed. Finally, it is worth noting that the sediment dynamics at Costa da Caparica beaches is intimately connected with the Tagus river inlet dynamics, with complex sediment exchanges between the beaches and the inlet southern sand banks (e.g., the Cachopo Sul sand bank) [17]. Possible causes for erosion at the Caparica beaches have been debated, amongst others, by Veloso-Gomes et al. [9,21], Silva et al. [10], Taborda and Andrade [27], and Fortunato et al. [17]. These point towards a combination of anthropogenic factors (sand extraction and river regulation) and natural agents (sea level rise, wave energy increase and shoreline rotation), which are not entirely understood. The modelled alongshore sediment fluxes are further discussed in Section 5.2.

Beach sediments consist of well-sorted medium-to-coarse sand (median grain size between 0.2 mm and 0.7 mm) [29]. At Costa da Caparica beaches, the dominant grain size is 0.3 mm. According to Freire [30], this sand is composed, predominantly, by siliceous grains and bioclasts.

The local closure depth was estimated according to Hallermeier [31] formula, using the onshore wave climate estimated at 14 m depth [28]. According to the original formula [31], this depth depends on the non-breaking significant wave height that is exceeded, on average, 12 h per year. This resulted in a value of 9.0 m at *São João da Caparica*, which is in agreement with beach cross-shore profile data from the COSMO monitoring programme [32], at *Praia de São João* and *Praia do Tarquínio*, from 2018 to 2021, that shows minor bathymetric changes at depths greater than −11 m (MSL) (approx. −8.7 m C.D.). The estimated closure depth increases to the south, and thus, the unique value of −12 m (MSL) was adopted for the entire coastal sector.

3. Data and Methods

3.1. Data

In the present analysis, aerial photographs, orthophotographs and topo-hydrographical surveys from 1979 to 2018 were used. Table 1 contains information on the data type, date and time of photo/orthophoto, scale, spatial range and tidal level. Regarding the spatial range, it covers either the total continuous sandy beach, from “*Cova do Vapor*” to “*Praia da Pipa*”, or just part of it, as indicated in each case. The total period was subsequently divided from 1978 to 2004 for model calibration, and from 2004 to 2018 for model performance verification.

These data were analysed with GIS-designated software, adopting the Official Portuguese reference system—PT-TM06/ETRS89—and the vertical Nautical Chart Datum, abbreviated as C.D., established 2.26 m below the present mean sea level (MSL) at Cascais [20]. Times of photos/orthophotos are referred to UTC (Coordinated Universal Time). Tidal levels were obtained using the “*Service Hydrographique et Océanographique de la Marine*” (<https://maree.shom.fr/>, accessed on 30 March 2023) tidal model estimates at Cascais.

Table 1. Aerial photographs, orthophotographs and topo-hydrographical surveys used in present study.

Data Type	Time and Date (dd/mm/yy)	Scale and Resolution (If Available)	Spatial Range	Tidal Level (m C.D.)
Aerial photo	7 April 1979; 11 h 00–12 h 00 (UTC + 1)	1:10,000	Entire sector	2.46–2.65
Topo-hydrographic survey	September and October 1979	1:5000	“Praia da Mata” to “Lagoa de Albufeira”	-
Topo-hydrographic survey	September 1980	1:2000	“Costa da Caparica”	-
Aerial photo	9 March 1989, 11 h 00–11 h 10 (UTC), 14 March 1989; 15 h 10 (UTC), 22 March 1989; 11 h 05 (UTC)	1:15,000	“Costa da Caparica” to “Lagoa de Albufeira”	0.74–0.85 1.67 1.66
Orthophotomap (False colour)	29 August 1995, (low-tide)	1:40,000 1 m resolution	Entire sector	1.0
Orthophotomap	9 November 2004, (high tide) 13 November 2004, (high tide) 14 November 2004, (high tide)	- 0.1 m resolution	Entire sector	3.2 3.7 3.5
Orthophotomap	6–7 September 2008, 15 September 2008, 10 October 2008	- 0.1 m resolution	Entire sector	-
Orthophotomap	24 October 2014, (high tide) 26 October 2014, (high tide)	- 0.1 m resolution	Entire sector	3.44 3.50
Orthophotomap	17 September 2018, (high tide)	- 0.03 m resolution	“Cova do Vapor” to “Praia da Cornélia”	2.7

3.2. Methods

3.2.1. Shoreline Identification

A mosaic for each collection of orthophotos/photos was constructed, and the shoreline was extracted. Several distinct shoreline indicators (e.g., [33]) can be obtained, but here, the use of a dynamic indicator was favoured, in line with the shoreline model assumptions, which was able to catch the annual and inter-annual variability. Moreover, not all photos allowed us to identify the high-tide water line. Hence, the wet/dry-sand line is the adopted proxy for the coastline or shoreline. In a recent work, Buccino et al. [34] used the instantaneous waterline. A single operator visually identified the shorelines for all data, thus avoiding any subjectivity associated with multiple operators.

An average beachface slope of 0.1 was assumed uniform for the whole sector, despite the occurrence of spatial and temporal variations [29], which would affect the shoreline position, albeit within the method’s accepted error (see below). Using the tidal level data at the time of the photo and the above beachface slope, all shorelines were transferred landwards or seawards to the mean sea level position, if in low tide or high tide, respectively. Wave runup was not accounted for, but it was checked that it would only affect minimally the results, within the methodology uncertainty.

For comparison and data analysis purposes, shoreline data points were extracted every 50 m along the baseline, as depicted in Figure 1.

Regarding the shoreline determination, a specific uncertainty or error analysis was not carried out here. Nevertheless, since the present analysis follows the procedure of Silva et al. [35], who performed an extensive error analysis, and uses similar data sources, we assume an identical error in the shoreline identification method, of the order of 3 m, not factoring in the tidal level adjustment. Moreover, according to the same authors [35], an uncertainty of a similar magnitude (circa 4 m) is associated with georeferencing the aerial photo mosaics. Combining these uncertainties, which sum non-linearly (the total uncertainty is equal to square-root of the sum of the, partial, squared uncertainties), results in an overall positioning root-mean-square error of circa 5 m [35], and thus, generally, the shoreline evolution is of significance only at places where this value is exceeded. Note

that although this error estimate may appear underestimated, given the methodological approximations and uncertainties, it is larger than that provided by other works using similar orthophotomaps (e.g., [34]), but it is similar to that obtained from air photos analysed by Hapke et al. [36]. Lastly, the correction for the tidal level adds an uncertainty, which sums linearly with the above. This is further discussed in Section 5.1.

3.2.2. Local Wave Climate

The wave climate at the closure depth (−12 m MSL) bathymetric contour, along the study area, was calculated using the SWAN (version 41.10) spectral wave model [37]. Sancho et al. [24] provide details of the model setting and application. In particular, the model was forced with spatial-uniform conditions at the domain western boundary, using the hindcast offshore wave climate time series at approximately 122 m water depth (hindcast data point located at 38°36' N and 9°33' W, WGS84 coordinate system), provided by Dodet et al. [38] and Dodet [25]. This time series consists of a 65-year hindcast data set, with data every 6 h, for the period from 1 January 1948 until 31 December 2012. Here, only the period from 1979 until 2012 was used.

The modelled results were compared with local measurements from a wave buoy placed at −22 m C.D. (38°37'33.6'' N and 9°23'16.8'' W, WGS84 coordinate system), at the mouth of Tagus estuary, for the period of 5 years, from 2007 until 2012. For a total of 4906 records, approximately equally distributed along the years, Sancho [28] obtained root-mean-square errors for the significant wave height, wave peak period and mean direction equal to 0.34 m, 2.08 s and 26°, respectively. The bias were −0.002 m, −0.222 s and −4.2°, respectively. These results are considered quite satisfactory, except for the wave direction mean-square error. Despite the latter appearing to be high, it is similar to the accuracy obtained for other wave model implementations (e.g., [17,39,40]), and thus, it was accepted. However, it cannot be ignored that $\pm 25^\circ$ errors in the wave direction can significantly affect the estimated longshore sediment transport fluxes and, presumably, the modelled shoreline evolution. According to Chataigner et al. [16], assuming that the one-line model is conceptually correct, a small wave angle bias (approximately 5–10°) has significant impacts on simulated long-term shoreline change trends. The lower bias obtained here for the wave direction indicates, however, that there should be no tendency along all the model results to underestimate or overestimate the wave direction (and alongshore sediment transport direction), and thus, one might expect that the modelling errors from this source should cancel out.

3.2.3. Shoreline Modelling

In the following, the shoreline evolution in the region of interest is modelled using the LITMOD model [41,42]. This is a classical one-line model, similar to the well-known GENESIS model [43], that allows us to easily define and evaluate scenarios, and to obtain medium-to-long-term (of the order of decades) estimates of the shoreline position for long (of the order of kilometres) coastal stretches. This model was designed to apply mostly to linear (or small-curvature) sandy beaches, where the shoreline evolution is mainly governed by the alongshore sediment transport and wave energy gradients, dependent on the local wave-breaking climate, sediment sources and sinks, sediment characteristics, cross-shore profile, coastal structures and boundary conditions. According to the model, at each time step, the shoreline moves parallel to itself, representing the movement of the entire beach profile (from the upper berm down to the closure depth), from the mass balance of the alongshore sediment fluxes and sediment sources/sinks. The model is presently prepared to deal with the effect of groins on the alongshore sediment fluxes, detached breakwaters, soft and hard coastal cliffs, and coastal revetments [41].

The wave-breaking characteristics are determinant to estimate the alongshore sediment fluxes. As the shoreline moves and rotates, the breaking wave properties (wave height and wave direction with the coast) alter iteratively, taking into account the breaking depth. The Kamphuis [44] formula was chosen to calculate the coastal alongshore sediment transport,

with the calibration dimensional transport coefficient k equal to 70% of the original value ($k_{\text{orig.}} = 2.3 \times 10^{-3} \text{ m}^{1.25} \text{ s}^{-2.5}$), in order to better fit the data. All simulations were carried out ignoring the tidal water level fluctuations, using a constant water level equal to the mean sea level.

According to the available data [29], the present model application considered a variable median grain size along the study area, increasing from north to south, from 0.27 mm to 0.75 mm. The Dean [45] equilibrium cross-shore profile form was adjusted to some profiles extracted from the 1980 hydrographic survey (identified in Table 1). Hence, at each alongshore position, depending on the sediment size, the cross-shore profile is given by $h = Ay^{2/3}$, with $A = 0.21D_{50}^{0.48}$, where h represents the water depth and y is the seaward distance from the water line. For $D_{50} = 0.32$ mm, the beach slope at the breaking zone is approximately equal to 1:30. Thus, in order to properly account for wave transmission around the groins, a locally adjusted beach profile was used. From the available topographic data, the beach crest height is at +4 m (MSL), and the depth of closure is 12 m (MSL), for the alongshore-averaged cross-shore profile. Thus, the active beach volume (per unit length) that moves back and forth parallel to the shoreline is 16 m in height. In the model setup, this height is further adjusted from north to south, stretch by stretch, allowing for a variation of that value by 94% to 115%, respectively. Hence, according to the data, the active profile height at the northern sectors is lower than that at the southern sectors.

For the numerical model, a 24 km reference or baseline was established, oriented N–20°-W, with origin at *Praia da Pipa* (Figure 1). All shoreline positions are measured relative to this reference, and a 50 m cell length was adopted, yielding a total of 456 points along the coast. Note that the cell length equals the data extraction spatial step, allowing for a direct comparison, without further data interpolations. Twenty-nine local wave climate points, approximately uniformly distributed along the coast, were considered for the model simulations. The model time step is 1.2 h. Northern and southern model boundary conditions were set such that the shoreline orientation is constant at each extremity.

Finally, the application of the proposed model to specific situations, such as the present one, requires the numerical model calibration and validation. The model calibration data and setup is further discussed in Section 5.1.

3.2.4. Local Coastal Protection Strategies

Table 2 contains 16 possible intervention strategies, planned with the Portuguese coastal management Authority (Portuguese Environmental Agency), for a period of 25 years. The management goals are halting beach erosion at Costa da Caparica beaches and protecting the city (people, property and economy) from wave overtopping and coastal flooding. Two distinct groups were conceived: the first (letter A) includes intervention strategies without any further hard engineering interventions (except for maintenance works of the present structures); the second group (letter B) contains alternatives with rearrangements of the present coastal structures, alone or complemented with beach nourishment operations. It is assumed that the present coastal revetment remains in place for all interventions. The groins mentioned in Table 2 are identified in Figure 3.

Scenario A1 corresponds approximately to the present (last decade) coastal management strategy, where Costa da Caparica beaches are nourished every 5 years with $1 \times 10^6 \text{ m}^3$ of sand, distributed along the coastal sector within $20,200 \leq x \leq 24,000$ m (see range in Figure 1). Scenario A2, albeit of minor intensity, is inspired by the strategy outlined by Duarte-Santos et al. [46], where it was recommended to perform a one-time, large volume, beach nourishment “shot” of $5 \times 10^6 \text{ m}^3$. Here, a volume of $3 \times 10^6 \text{ m}^3$, instead of $5 \times 10^6 \text{ m}^3$, was suggested by the Portuguese Environmental Agency. Scenario A3 was defined mainly for comparison purposes, in terms of what would happen if no action were taken. Scenario A4 is similar to A1, except that the nourishment is confined to a shorter alongshore area, within groins EC1 to EC7 ($20,750 \leq x \leq 22,650$ m).

Table 2. Coastal intervention scenarios.

Scenario	Description
A	Without hard engineering interventions
A1	1 × 10 ⁶ m ³ beach nourishments, every 5 years, distributed alongshore over 3800 m
A2	One large (3 × 10 ⁶ m ³) beach nourishment “shot”, at project beginning lifetime
A3	No intervention
A4	1 × 10 ⁶ m ³ beach nourishments, every 5 years, distributed alongshore over 1900 m
B	With hard engineering interventions
B1	Similar to A1; removal of all groins from EC1 to EC7
B2	Similar to A1; removal of groins EC2, EC3, EC5, EC6 and EC7
B3.1	Similar to B1; EV1 groin length increase of 100 m
B3.2	Similar to B1; EV1 groin length increase of 200 m
B3.3	Similar to B1; EV1 groin length increase of 300 m
B4.1	Similar to A1; EV1 groin length increase of 100 m
B4.2	Similar to A1; EV1 groin length increase of 200 m
B4.3	Similar to A1; EV1 groin length increase of 300 m
B5.1	Similar to A3; EV1 groin length increase of 100 m
B5.2	Similar to A3; EV1 groin length increase of 200 m
B5.3	Similar to A3; EV1 groin length increase of 300 m
B6	Similar to A1; removal of groins EC1, EC2, EC4, EC6 and EC7; EV1 groin length increase of 300 m

The second group comprises strategy B1, which equals A1 in terms of beach nourishment, but accounts for the removal of all groins in front of Costa da Caparica, retaining the ones at *Cova do Vapor* (at the northern limit of the coastal arch), namely, groins EV1 and EV2. Hence, A1 versus B1 shall allow us to understand the capacity of the groins in retaining the added sand. Scenario B2 is similar to A1 and B1 regarding the nourishments, but it considers removing groins EC2, EC3, EC5, EC6 and EC7.

An extension of the groin at the northern end of this coastal sandspit has been debated for a long time [47] and is thus evaluated here, in comparison with other alternatives. Hence, simulated interventions B3.1, B3.2 and B3.3 are all similar to B1, but they include an extension of groin EV1 by 100, 200 and 300 m, respectively. Alternatives B4.1, B4.2 and B4.3 include, likewise, the same expansions of groin EV1, but they are otherwise similar to strategy A1 (present management option), i.e., all present structures would be maintained, and beach nourishment would be performed. The combination of no-nourishment (A3) with the EV1 groin expansions results in scenarios B5.1, B5.2 and B5.3. Finally, scenario B6 considers removing groins EC1, EC2, EC4, EC6 and EC7, beach nourishments equal to A1 and a 300 m increase in groin EV1.

All the above intervention scenarios were independently configured into LITMOD, and the shoreline evolution was simulated for a period of 25 years, starting from the position measured in 2018. The forecast-period wave climate in the model was the same as the wave climate series from 1979 to 2004. The comparison between the different interventions will focus in Costa da Caparica frontal and adjacent beaches, bounded by 20,000 ≤ x ≤ 24,000 m. This is the region where present interventions take place and where coastal erosion and wave overtopping are problematic.

4. Results

4.1. Calibration and Verification

Figure 4 shows the simulated shoreline position at 2004 (after 25 years of simulation) for the entire study area, after model calibration, in comparison with the measured line. Vertical and horizontal scales are distorted. One generally notes good agreement over the entire coastal arch, except at the southern, first 1000 m, where the model predicts shoreline

retreat, which is not observed in the data. The modelled–observed discrepancy is close to 150 m in that sector, but it is as low as 6 m in some of the northern groin-confined Costa da Caparica beaches.

The average measured shoreline movement for the entire study area, excluding the profiles where the difference between the two lines was less than 5 m (the method’s precision), was 0.09 m/year, corresponding to accretion. This value matches satisfactorily the value of 0.14 m/year obtained by Silva et al. [48], using other shoreline indicators, for the period 1980–2005. Despite the overall slight accretion for the entire sandy stretch, erosion was significant at the northern 3 km-long stretch, reaching a localised maximum of approximately −100 m (−4 m/year).

Table 3 provides the average shoreline advance or retreat, measured and modelled, between 1979 and 2004, for six sectors (A to F; see location in Figure 4) along the studied sandy coast for both the measured and simulated results. The difference between data and model results are minimal and within the accepted data precision (see Section 3.2.1) for sectors C and F. It is also slightly above that value for sector D. Disparities in sectors B and E are around 30 m. Sector A, at the southern extremity, is the one where discrepancies are the greatest, most likely due to an inadequate southern boundary condition for the sediment dynamics at this study site. However, errors in the wave direction estimation and its effect on shoreline modelling cannot be neglected [16], but they also cannot be appraised since no wave monitoring data exist at the coast.

Table 3. Difference between final (2004) and initial (1979) shoreline positions in the calibration period (in meters), spatially averaged by coastal stretch (A to F, from south to north).

	A 1500 < x ≤ 2000 (m)	B 2000 < x ≤ 7000 (m)	C 7000 < x ≤ 14,000 (m)	D 14,000 < x ≤ 17,000 (m)	E 17,000 < x ≤ 20,700 (m)	F 20,700 < x ≤ 24,000 (m)
Simulated	−159.6	−29.8	3.5	11.5	−25.2	−14.7
Measured	−33.8	2.0	4.7	17.2	4.9	−19.4

The calibrated model was further verified against field data for the period 2004 to 2018. It is noted that in 2005–2006, the coastal structures at the northern sector (Costa da Caparica beaches) were rearranged relative to the previous configuration [21], so the new arrangement was set-up in the model. Furthermore, four nourishment operations (from 2007 to 2014, [19]) were introduced in the model, simulating as closely as possible the nourished volumes, locations and periods of interventions. The total added sand was $3.5 \times 10^6 \text{ m}^3$. Since the wave climate had only been determined until 2012, and it remained relatively stable during the period 1979–2004 [28], i.e., without any noticeable tendency for long-term variation, it was decided that the wave time series used in the calibration period would be used in the verification period.

Figure 5 compares the shoreline position in 2018 using the previously calibrated model (left) with that obtained after a finer re-calibration setting (right), for the northern 4 km-long stretch (covering mainly sector F), where all past coastal works and beach nourishment interventions occurred. A better match is observed for the post-verification model configuration, particularly at the northern beach (“Praia de São João”). In that beach, the root-mean-square difference between modelled and measured coastlines were 50.1 m and 35.6 m for the post-calibration and post-verification model settings, respectively. The largest differences between modelled and measured shorelines are visible at the groin-confined beaches, where the model is unable to properly simulate the diffraction processes leeward of the groins (e.g., [49]), and generally predict a greater shoreline erosion than that measured. It is noted that the recalibration process was for the entire coastal arch, but the aim was to achieve a better match at the Costa da Caparica beaches (sector F of Table 3), where the different management strategies will be compared.

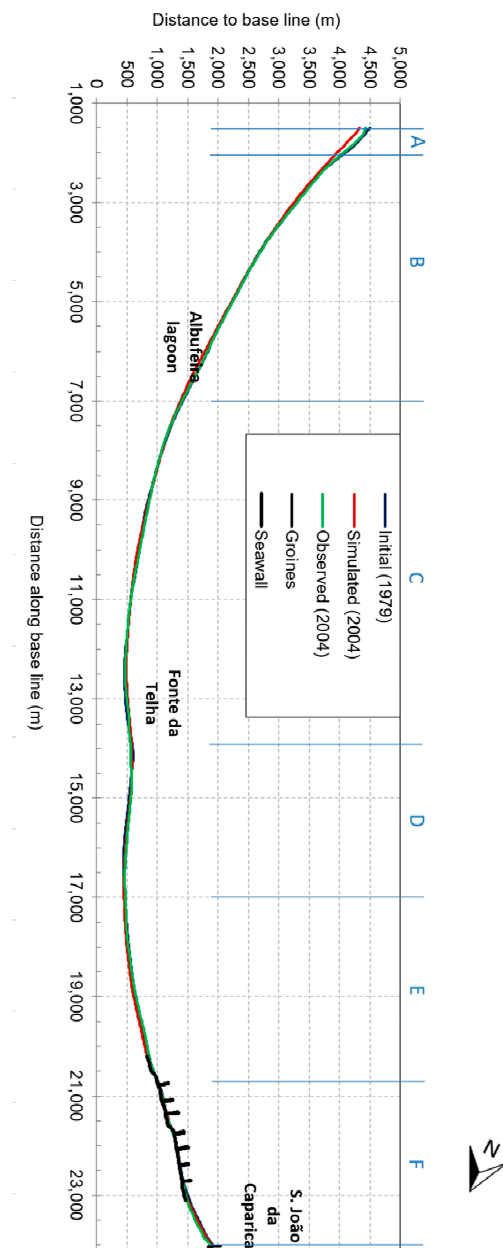


Figure 4. Modelled (calibrated; red) and measured (green) shoreline positions in 2004 over the entire study area. Initial shoreline configuration in 1979 (dark blue) and hard structures (groynes and coastal revetment; black). The limits of the sectors referred to in Table 3 are marked in light blue, at the top.

4.2. Coastal Intervention Scenario Simulations

4.2.1. Soft Solutions Plus Present Coastal Structures (Group A)

Figure 6 compares the predicted shoreline positions 20 years past the initial 2018 configuration, for all soft intervention strategies (group A in Table 2). Solution A3 (“no intervention”) is, clearly, the one that allows for the largest coastal erosion at this sector. On the contrary, alternatives A1 and A4 induce slight coastline advances, particularly at some of the pocket beaches and *Praia de São João* (between EC7 and EV1). This is confirmed in Figure 7, which shows the time-evolution of the averaged shoreline advancement or retreat for these interventions, within the region $19,500 \leq x \leq 24,000$ m. Strategy A2 also induces overall shoreline retreat at this sector, which might be explained by the fact that this strategy adds to the system, in 25 years, less sediment ($3 \times 10^6 \text{ m}^3$) than strategies A1 and

A4 (totalizing $5 \times 10^6 \text{ m}^3$). A second reason is related to the fact that, for A2, the volume is placed only once, at the project start, and thus, its long-term effect is less noticeable.

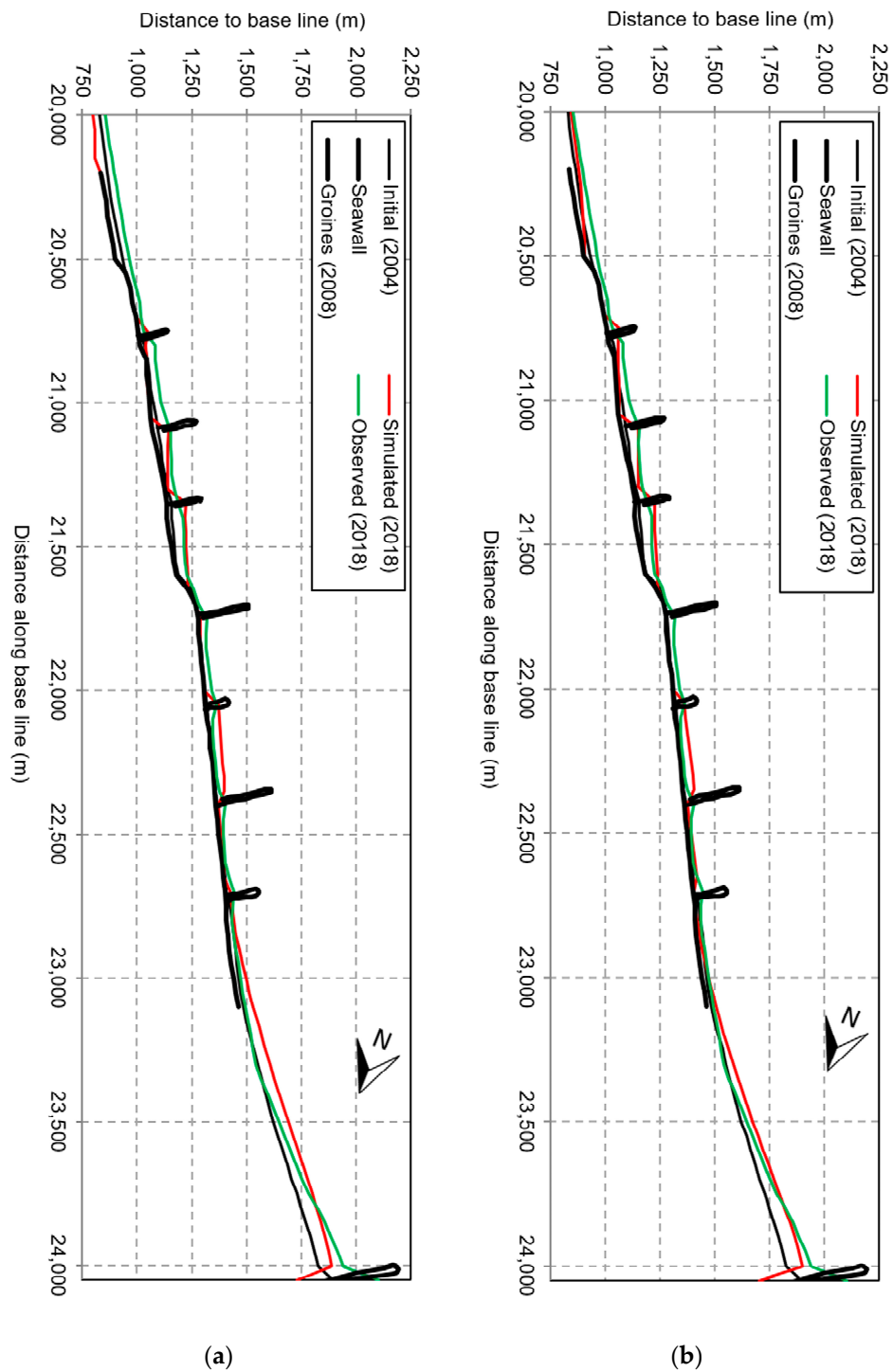


Figure 5. Modelled (red) and measured (green) shoreline positions in 2018 at Costa da Caparica beaches. Initial shoreline configuration in 2004 (black thin line) and hard structures (groins and coastal revetment; black thick line). (a) Results from post-calibration simulation; (b) results from post-verification simulation.

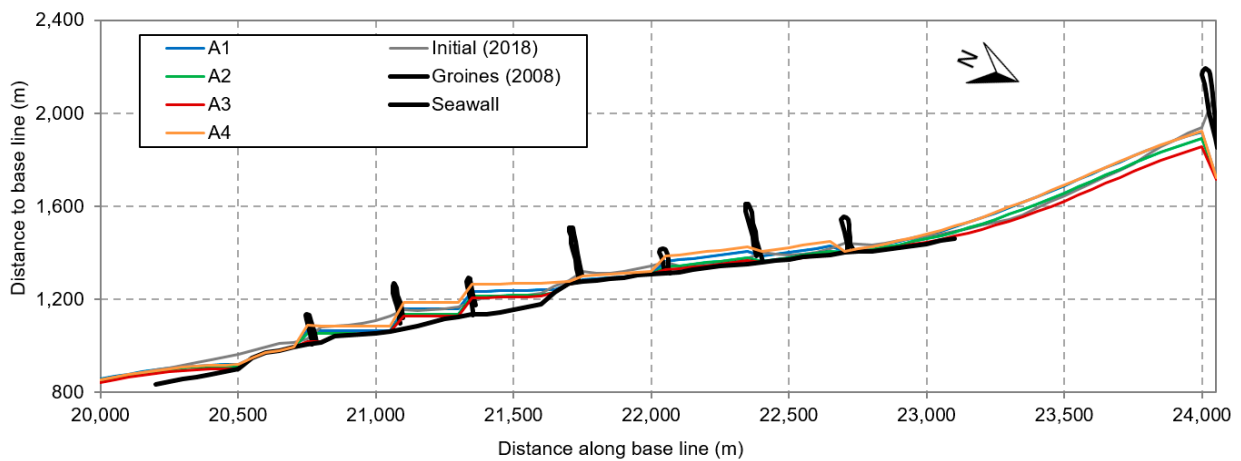


Figure 6. Modelled shoreline positions 20 years past initial configuration (2018) at Costa da Caparica beaches for intervention strategies A1, A2, A3 and A4.

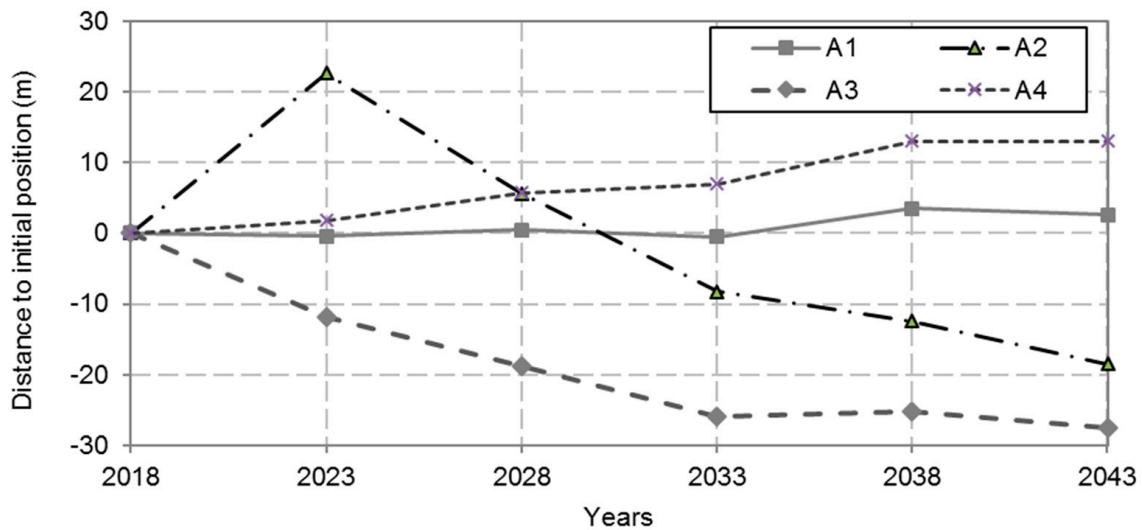


Figure 7. Time-evolution of mean shoreline position relative to initial position at Costa da Caparica beaches for intervention strategies A1, A2, A3 and A4.

4.2.2. Structural Interventions, with or without Soft Solutions (Group B)

Figure 8 shows the shoreline positions after a simulation of 20 years for all the group B intervention scenarios. The top sub-figure compares strategies B1, B2, B6 and A1, evidencing that the removal of several intermediate groins (e.g., strategies B1 and B2) reduces the sand accumulation capacity of the groin-confined beaches (comparing to strategy A1). Strategy B2 shows also that retaining groin EC1 (the southern-most groin) allows for removing EC2 without beach loss between EC1 and EC3. The results for strategy B6 show that the increase in EV1 provides a significant positive impact in retaining sand from EC6 to EV1 ($22,400 \leq x \leq 24,000$ m). For all these scenarios, the shoreline positions between EC4 and EC6 nearly coincide with the coastal revetment alignment, indicating thus a very narrow beach.

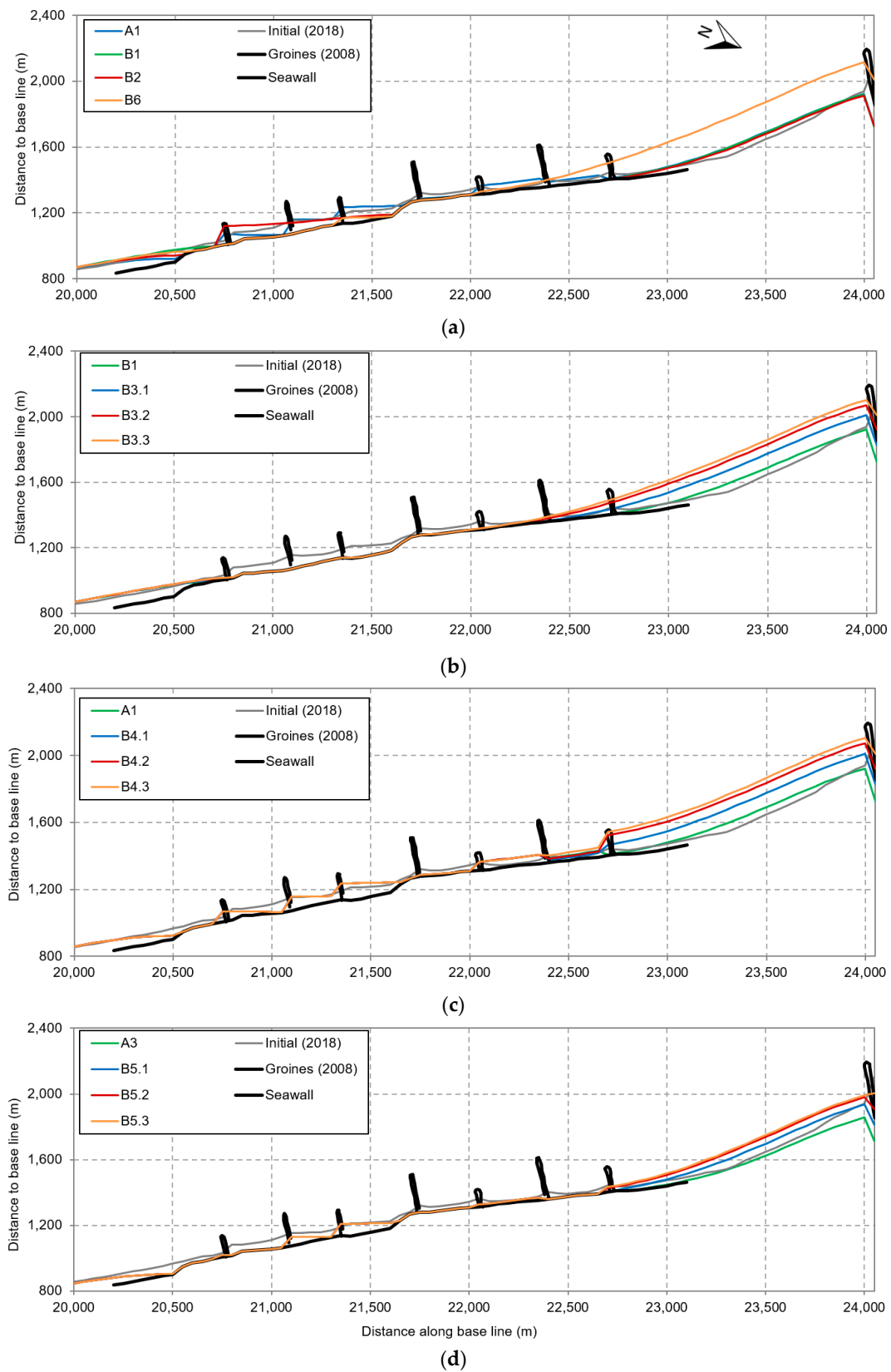


Figure 8. Modelled shoreline positions 20 years past initial configuration (2018) at Costa da Caparica beaches for intervention strategies: (a) A1, B2, B2 and B6; (b) B1, B3.1, B3.2 and B3.3; (c) A1, B4.1, B4.2 and B4.3; (d) A3, B5.1, B5.2 and B5.3.

The results for the scenarios considering the removal of all groins from EC1 to EC7 (B1 and B3) are given in Figure 8b. It is clear to observe the beneficial effect of increasing the terminal groin EV1 (simulations B3), which is able to trap the northward (down-drift)-directed sediment flux, proportionally to its length increase. This beach widening is limited, at best, to $x \geq 22,400$ m, that is, northward of the present position of groin EC6. Southward of this position, predictions show the shorelines attaching to the seawall, thus reducing the beach width to nearly zero. Figure 8c evidences again the positive effect of EV1 groin increase (scenarios B4), in addition to maintaining the present strategy (A1).

Figure 8d compares results without any intervention (A3) with a similar set but considering the length expansion of groin EV1 (B5). As in Figure 8c, differences between all modelled shorelines are only discernible at *Praia de São João*. Even without beach nourishment, the EV1 groin extension is effective in retaining sediments in that beach that would otherwise by-pass the present groin.

Figure 9 shows the time-evolution of the sector-averaged shoreline advance or retreat, within the sector $19,500 \leq x \leq 24,000$ m, for all group B interventions. Overall, strategies B3.3, B4.3 and B6, all corresponding to a 300 m increase in groin EV1 together with beach nourishment, are the ones that promote the most noticeable beach accretion. Strategy B5 does not generally allow for beach growth. For the same EV1 groin increase, strategy B4 is generally slightly more positive than B3; that is, retaining the present Costa da Caparica groins (EC1 to EC7) promotes more accretion than removing them. This is also observed by comparing results of A1 with B1 (Figure 9a).

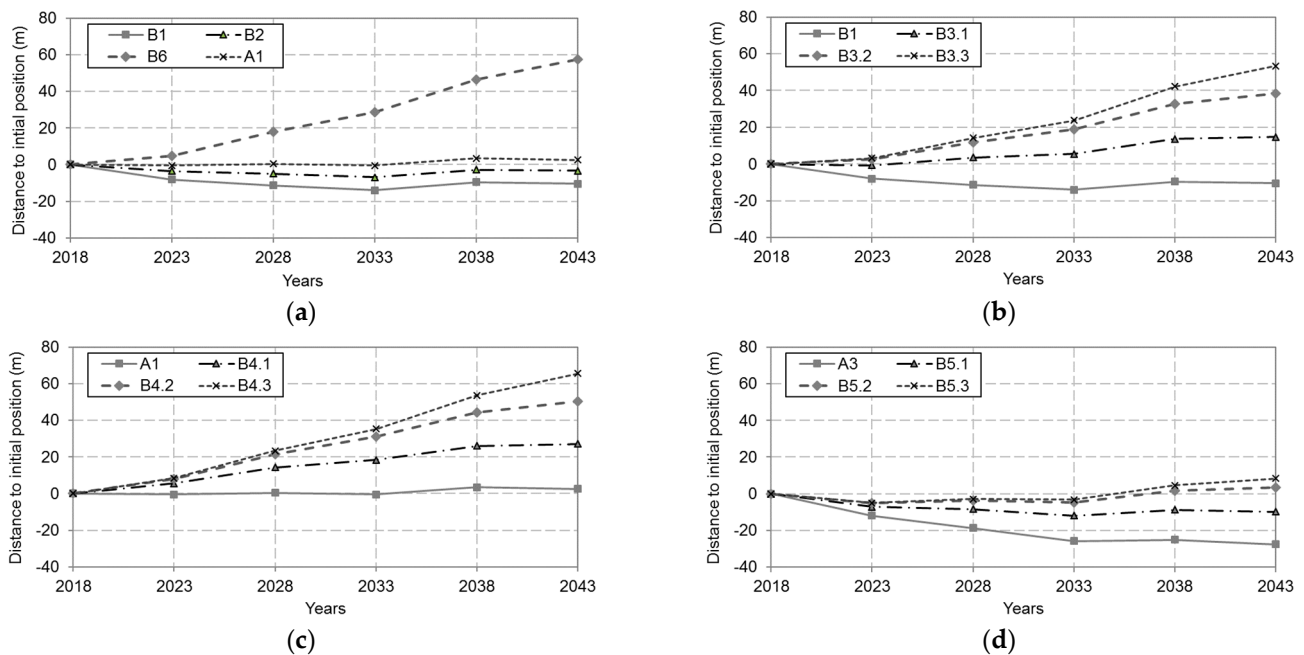


Figure 9. Time-evolution of mean shoreline position relative to initial configuration at Costa da Caparica beaches for intervention strategies: (a) A1, B1, B2 and B6; (b) B1, B3.1, B3.2 and B3.3; (c) A1, B4.1, B4.2 and B4.3; (d) A3, B5.1, B5.2 and B5.3.

5. Discussion

5.1. One-Line Model Calibration Data and Setup

A brief discussion on one-line model limitations is provided by Chataigner et al. [16], who highlight the role of the active profile depth, the assumption of a constant equilibrium profile and the use of k as a calibration parameter in the longshore transport rate. The one-line model approach depends on the quality of both the input data and the choice of model free parameters. Depending on the inherent complexity of the study site and the quality of the input data, the one-line longshore model may generate changes in the beach

planform (e.g., reorientation) that are different from observations [16]. Hence, the issues of model implementation and limitations are discussed here.

The measured shoreline movement displayed in Figure 4 and characterised in Table 3 relate to the comparison between the positions in April 1979 and November 2004. As these dates refer to different maritime wave regimes (post-winter energetic versus post-summer low-energy seasons), the seasonal cross-shore profile-shaping processes can induce shoreline movements at this coastal sector of up to circa 20 m (this number results from the analysis of 2018–2021 cross-shore profile data, at *Praia de São João* and *Praia do Tarquínio*, available from the monitoring programme COSMO [32]). Hence, their absolute inter-comparison for estimating long-term shoreline movement rates could lead to erroneous interpretation. However, the seasonal behaviour of the coastline does not affect the model calibration, as the input-modelling conditions reproduce the wave time series and shoreline position from a given start date to a given end date, regardless of their seasons. This is also acknowledged by Chataigner et al. [16], who state that over long time-scales (e.g., interannual to decadal) longshore processes become increasingly important.

A shoreline determination precision of ± 5 m was estimated in Section 3, based on the analysis carried out by Silva et al. [35]. The shoreline determination procedure included a correction for the tidal level, at the time of data acquisition, which adds more uncertainty to the above precision. The beach profile, particularly at the northern sector of the study site, changes its slope from the upper to the lower foreshore. Using data from the COSMO monitoring programme [32], at *Praia de São João* and *Praia do Tarquínio*, the average upper-foreshore (medium-to-high tide water line) slopes are circa 0.12 and 0.09, respectively. These numbers are in accordance with the average beachface slope of 0.1, used before. However, the average lower foreshore (medium-to-low tidal levels) slopes are 0.04 and 0.033, respectively, at the same profiles. Thus, the horizontal correction of the shoreline position needed to be larger if below mean tidal level at the time of data acquisition. This did not occur for the aerial photos and orthophotos of 1979, 2004 and 2018 (see Table 1), as all times corresponded to instants where the waterline was in contact with the upper foreshore. Hence, using the average high-tide level of the 2004 orthophoto (3.5 m C.D.), the error associated with the tidal correction is of the order of $((3.5 - MSL)/slope) - (3.5 - MSL)/0.1$, where *slope* is the true upper beachface slope. Using *slope* = 0.12 yields an error of 2.5 m. A lower value is obtained for the 1979 dataset, as the tidal level was lower (but above mean sea level). This highlights the validity of the tidal-level shoreline correction procedure. We note that more care in the correction procedure would be needed in case of the 1989 and 1995 datasets, obtained at low-tide phases, but not used for the present model calibration.

The 1980 topo-hydrographic survey was chosen for model calibration, since this survey lies within the calibration period (1979–2004), and should, therefore, represent adequately the beach profile characteristics for that period. The data used herewith was extracted from 1 m-apart bathymetric contours, which are rather crude and thus of questionable quality. These data were thus compared with recent, 2018–2021, multi-beam, topo-hydrographic profiles collected at *Praia de São João*, from the COSMO programme [32]. The comparison indicates that the 1980 lower-resolution profiles can also represent the present beach profiles, the major difference being a slightly larger foreshore volume, which is explained by the beach being more robust, prior to the long-term erosion that occurred until the first beach nourishment operations.

The study site description in Section 2 indicates that the sandy stretch is somewhat non-homogeneous (e.g., the spatial grain size variation [29]) and long, possibly reducing the validity of the LITMOD (one-line) model application. However, the model parametrization and setup used here, namely, the alongshore variable grain size, variable beach profile and variable active beach volume (both varying sectorially, in a total of five sectors), allowed us to account for that non-homogeneity.

Further, in relation to the study site length and curvature, one-line models are valid to limited (small) shoreline curvatures, usually due to the decoupling of the wave refraction

and shoreline movement computations [50]. In the present case, the one-line model baseline is closer to the shore-parallel configuration at the northern extremity than at the southern (Figure 1), and the shoreline presents a small curvature. This configuration ensures a potential low error due to those effects at the northern sector, where the coastal protection strategies are inter-compared. The greater model-data discrepancy found at the southern extremity in the model calibration phase (Figure 4) may also be due to this effect.

The data at the northern sector indicates that there is a clear long-term trend in shoreline behaviour. The assumption of a clear trend implies that the wave action producing longshore sand transport and boundary conditions are the major factors controlling long-term beach change [51]. A model-data comparison in the calibration stage (Figure 4) allowed us to conclude that the northern boundary condition was appropriate, unlike the southern one. Other southern boundary conditions were tested, providing poorer results. This is further discussed in the next section.

The Kamphuis [44] formula for the alongshore transport rate is a function of the (along-shore varying) breaking wave height and wave direction. A commonly used alternative transport formula is the CERC formula [51]. Most often, for both formulae, the transport coefficient k is used as a calibration parameter (e.g., [51–53]). For example, Hanson and Kraus [51] refer a common range of 75 to 100% of the original k value, for the CERC formula. Pilkey and Cooper [54] refer to the use of a much broader range, with k values from 2 to 300%. Considering the above, the value of k used in the present model configuration is quite acceptable and enabled us to obtain a satisfactory calibration. Since this affects the transport magnitude uniformly, the beach alongshore variability was accounted for through the other model configurations, already mentioned.

5.2. Alongshore Sediment Fluxes

The discrepancy of the predicted versus measured coastlines at the southern extreme of this coastal sector, in the calibration phase (Figure 4), relates to an over-estimation of the sediment flux at that boundary. In the calibration and verification phases, the averaged net transports at the model boundary, $x = 1500$ m, were 160×10^3 m³/year and 200×10^3 m³/year, respectively, directed southward. For the intervention scenarios, the flux resulted equal to 167×10^3 m³/year for all simulations. These estimated fluxes are not corroborated by data and result from an ineffective model boundary condition. This may be due to the existing headland circa 650 m north of the sandy beach southern extreme, which is likely to act to stabilize the southern beach (*Praia da Pipa*), which was not included in the model setup. One other reason may be related to the fact that the sediment characteristic dimension (D_{50}) is much larger at that extreme (>0.75 mm), and despite the model accounting for a variable alongshore grain size, the used simplification could not exactly reproduce the reality. Nevertheless, the effect of this exaggerated net sediment flux at the southern extreme propagates only to approximately 5000 m, northward, in the model domain (Figure 10). Indeed, the net averaged sediment fluxes in the region $x > 5000$ m is limited to approximately $\pm 50 \times 10^3$ m³/year (Figure 10). This net flux results, generally, from the balance between a 5-to-20-times-larger bulk transport, northward or southward directed, except at Costa da Caparica beaches ($20,000 \leq x \leq 23,000$ m), where the groins limit these fluxes. For $x > 5000$ m, it is also observed that the net flux varies alongshore from positive (southward) to negative (northward), and is negative at Costa da Caparica beaches.

The averaged net sediment transport at the northern extremity was -50×10^3 m³/year and -116×10^3 m³/year in the calibration and verification phases, respectively. These fluxes are within the known estimates of data-inferred alongshore values at *Praia de São João*, which are of the order of -200×10^3 to -275×10^3 m³/year [55,56], and other model estimates [57].

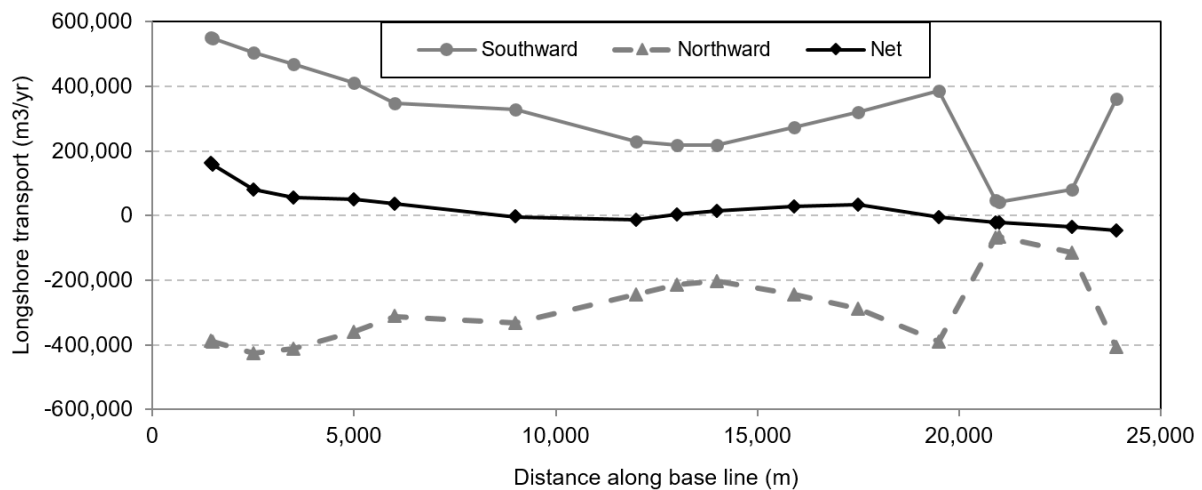


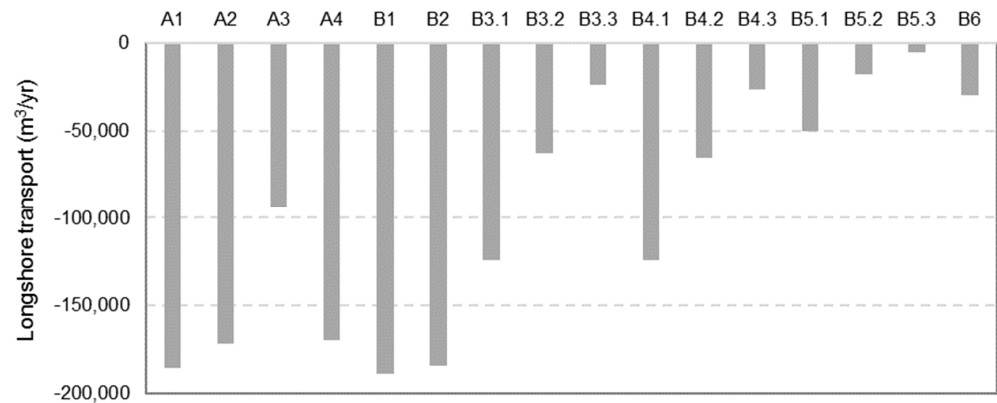
Figure 10. Alongshore annual mean sediment flux spatial distribution, for the post-calibration model simulations (1979–2004).

Figure 11 shows the annual mean net sediment fluxes for all intervention scenarios (see Table 2) at groin EV1 cross-section ($x = 24,000$ m) and immediately south of Costa da Caparica beaches ($x = 19,500$ m). For all soft-intervention simulations (group A), the predicted fluxes at EV1 ranged from $-170 \times 10^3 \text{ m}^3/\text{year}$ to $-185 \times 10^3 \text{ m}^3/\text{year}$, except for scenario A3—no beach nourishment—where the flux was smaller due to the scarcity of sediments to transport. Figure 11a further evidences the expected reduction in the net alongshore sediment transport as the terminal groin EV1 length increases. Scenario B5.3 is the one with the least amount of mean annual sediment ($-5.2 \times 10^3 \text{ m}^3/\text{year}$) bypassing EV1, followed by scenarios B5.2 ($-17.6 \times 10^3 \text{ m}^3/\text{year}$) and B3.3 ($-23.8 \times 10^3 \text{ m}^3/\text{year}$). At $x = 19,500$ m, the annual-averaged sediment fluxes are much smaller, and, depending on the intervention strategy, the flux towards the coastal cell comprising Costa da Caparica beaches can be either positive or negative (Figure 11b). We note that this cross-section corresponds roughly to the one where the annual mean alongshore net sediment flux changes its direction, in the calibration simulation (see Figure 10). Figure 11b also shows that interventions B1, B2, B3 and B6 induce positive (southward) net fluxes, that is, promoting the removal of sediments from Costa da Caparica beaches. On the contrary, strategies A3 and B5 (both without beach nourishment) mobilise significant sediment fluxes from the south (northward), in an attempt to feed the starving beaches at the north. Intervention scenarios A1, A2, A4 and B4 are the ones with the smallest net fluxes, with A4 being preferable because it promotes sediment into Costa da Caparica cell.

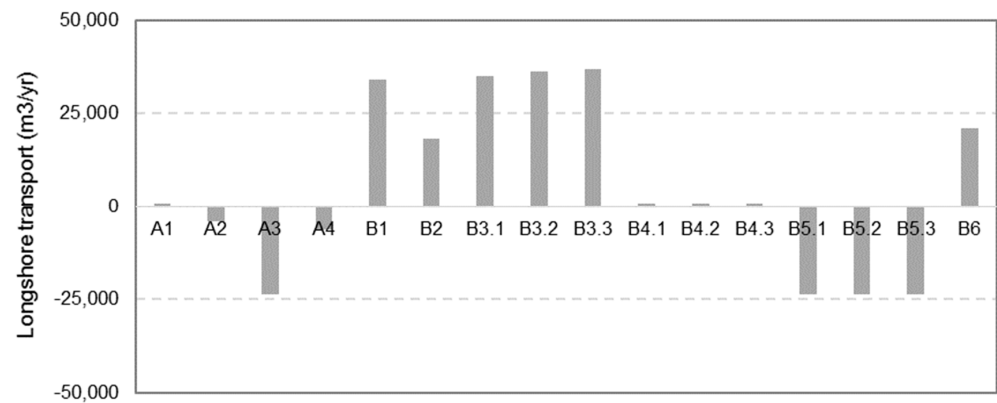
5.3. Sediment Volume Budget

The accumulated sediment budget at the littoral cell of Costa da Caparica beach (between sections $x = 19,500$ m and $x = 24,000$ m) was determined from the computed alongshore sediment fluxes at the boundary sections and the overall projected sand nourishments, for the 25-year projection lifetime. Figure 12 (grey bars) compares these results for the 16 intervention scenarios (see Table 2). The total nourishment for each strategy is also presented (dashed-pattern bars) as well as the final alongshore average shoreline movement (orange line, positive corresponds to accretion). In relation to the overall sediment budget, strategy A4 is, amongst the non-structural interventions (group A in Table 2), the most efficient in retaining sediment. All the others (A2 and A3), except for A1, result in less sediment in the cell than at the initial condition. Strategies B1 and B2, which are similar to A1 but include the removal of some groins, also induce sediment losses. As shown previously, the lengthening of groin EV1 (see Figure 3) in strategies B3 and B4 contributes significantly to sediment accumulation. Accordingly, strategy B4.3 causes the largest sediment retention in the system, nearly preserving all the sand added to the system. Naturally, since the average shoreline displacement is proportional to the accumulated

volume, those two curves follow the same tendency in Figure 12. The largest average beach growth is 65.6 m for scenario B4.3, and the continuation of the present strategy (A1) results in an accretion of only 2.6 m.



(a)



(b)

Figure 11. Annual mean net sediment fluxes for all intervention scenarios at: (a) $x = 24,000$ m; (b) $x = 19,500$ m.

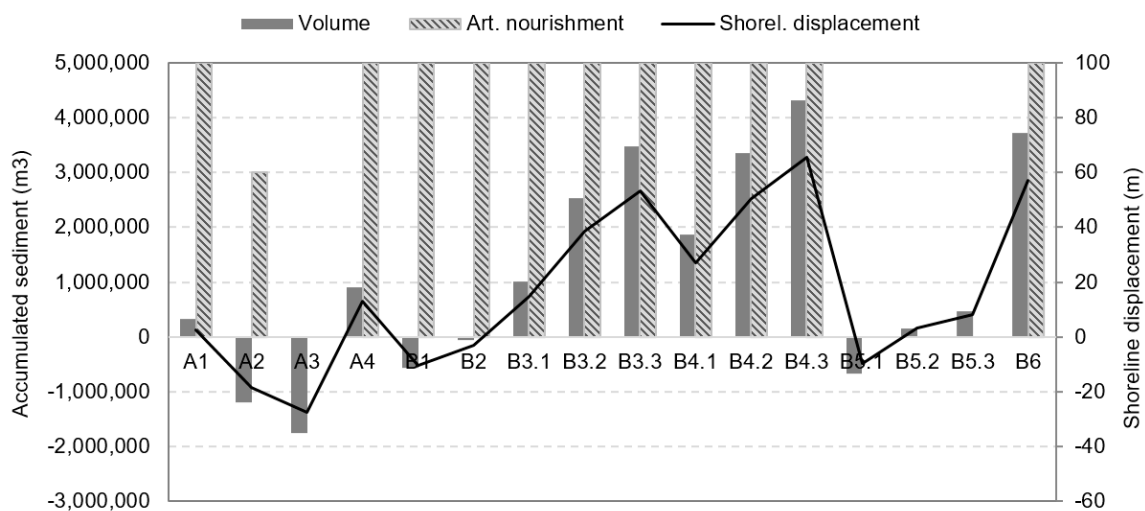


Figure 12. Accumulated sediment budget, artificial nourishments and average shoreline advance/retreat at Costa da Caparica cell (comprised within $19,500 \leq x \leq 24,000$ m), for the various intervention strategies.

6. Conclusions

Costa da Caparica beach, in Portugal, has been subject to coastal erosion over the past 70 years (e.g., [10]). This chronic situation led, in the period 2004–2006, to reconstructing and reshaping the previously erected groins and to strengthening the seawall [9]. This action was followed by a succession of five beach nourishment interventions in 2007, 2008, 2009, 2014 and 2019, feeding to the beach a total of 4.5×10^6 m³ of compatible sand [58,59]. This paper compares the present management strategy with 15 alternative ones (Table 2), also based on beach nourishment interventions, some combined with coastal structures interventions. These intervention scenarios were compared in terms of shoreline advance or recession for a period of 25 years, using a classical one-line shoreline evolution model [41,42].

The results indicate that the present management strategy (designated by A1) is effective in holding the shoreline position, although a similar strategy (A4), deploying the same overall sediment volume but over a shorter area, could lead to slightly better results (Figures 6 and 12). The best options, which are capable of promoting beach accretion at Costa da Caparica beaches, implicate the lengthening of groin EV1 (shown in Figure 3), north of *São João da Caparica*. The longer the increase in groin EV1, the greater the beach sediment volume gain, moved by littoral drift, at the Costa da Caparica beaches. However, such an intervention would need a detailed assessment of the hydro- and sediment dynamics changes at the Tagus river mouth and adjacent beaches.

All other assessed coastal engineering strategies (A2, A3, B1, B2 and B5) are not only incapable of increasing the beach width but also lead to even narrower beaches than the baseline solution (A1). Of all the intervention scenarios, the one associated with maintaining the present beach nourishment strategy and increasing the terminal groin EV1 by 300 m (B4.3) promotes the largest sediment retention in the upper beach and foreshore, nearly preserving all the sand nourishment provided to the system. Additionally, it is also concluded that groins EC1, EC2, EC4, EC6 and EC7 are not strictly necessary to the beach alongshore equilibrium, as intervention strategy B6 leads to a nearly similar beach accretion as strategy B4.3.

Lastly, one concludes that shoreline evolutions models can be used with success in comparing coastal management alternatives, provided they are properly calibrated with site data. Here, the results at Costa da Caparica beaches are in accordance with the present knowledge of the beach sediment dynamics.

Funding: This research was conducted within a contract coordinated by the Portuguese Environmental Agency and co-funded by the Portuguese “POSEUR—Programa Operacional Sustentabilidade e Eficiência no Uso de Recursos” (reference POSEUR-02-1809-FC-000039).

Data Availability Statement: Not applicable.

Acknowledgments: The author acknowledges the Portuguese Territorial General Directorate (DGT) for making available the orthophotos, the Portuguese Environmental Agency for supporting this study, and Dodet et al. (2010) for providing the hindcast offshore wave data. Discussions with Celso Pinto and Luís Portela were very fruitful in defining the intervention strategies evaluated here. Vitor Pisco helped with the model setup and runs. The data collection programme “Monitoring of the Portuguese continental coastal zone” (COSMO, [32]) was financed by the POSEUR funding programme (“Operational Programme for the Sustainability and Efficiency of the Resources Expenditure”). The manuscript revision by Óscar Ferreira and the anonymous reviewers is greatly appreciated.

Conflicts of Interest: The author declares no conflict of interest.

References

1. Pranzini, E. Coastal erosion and shore protection: A brief historical analysis. *J. Coast. Conserv.* **2018**, *22*, 827–830. [CrossRef]
2. Mentaschi, L.; Vousdoukas, M.I.; Pekel, J.; Voukouvalas, E.; Feyen, L. Global long-term observations of coastal erosion and accretion. *Sci. Rep.* **2018**, *8*, 12876. [CrossRef]
3. Vousdoukas, M.I.; Ranasinghe, R.; Mentaschi, L.; Plomaritis, T.A.; Athanasiou, P.; Luijendijk, A.; Feyen, L. Sandy coastlines under threat of erosion. *Nat. Clim. Chang.* **2020**, *10*, 260–263. [CrossRef]

4. Petropoulos, A.; Kapsimalis, V.; Evelpidou, N.; Karkani, A.; Giannikopoulou, K. Simulation of the Nearshore Sediment Transport Pattern and Beach Morphodynamics in the Semi-Enclosed Bay of Myrtilos, Cephalonia Island, Ionian Sea. *J. Mar. Sci. Eng.* **2022**, *10*, 1015. [[CrossRef](#)]
5. Hinkel, J.; Lincke, D.; Vafeidis, A.T.; Perrette, M.; Nicholls, R.J.; Tole, R.S.J.; Marzeiong, B.; Fettweis, X.; Ionescu, C.; Levermann, A. Coastal flood damage and adaptation costs under 21st century sea-level rise. *Proc. Natl. Acad. Sci. USA* **2014**, *111*, 3292–3297. [[CrossRef](#)]
6. Gracia, A.; Rangel-Buitrago, N.; Oakley, J.A.; Williams, A.T. Use of ecosystems in coastal erosion management. *Ocean. Coast. Manag.* **2018**, *156*, 277–289. [[CrossRef](#)]
7. Sánchez-Arcilla, A.; García-León, M.; Gracia, V.; Devoy, R.; Stanica, A.; Gault, J. Managing coastal environments under climate change: Pathways to adaptation. *Sci. Total Environ.* **2016**, *572*, 1336–1352. [[CrossRef](#)]
8. Ferreira, J.C.; Cardona, F.S.; Jóia-Santos, C.; Tenedório, J.A. Hazards, vulnerability, and risk analysis on wave overtopping and coastal flooding in low-lying coastal areas: The case of Costa da Caparica, Portugal. *Water* **2021**, *13*, 237. [[CrossRef](#)]
9. Veloso-Gomes, F.; Costa, J.; Rodrigues, A.; Taveira-Pinto, F.; Pais-Barbosa, J.; Neves, L. Costa da Caparica artificial sand nourishment and coastal dynamics. *J. Coast. Res.* **2009**, *56*, 678–682.
10. Silva, R.; Veloso-Gomes, F.; Pais-Barbosa, J. Morphological Behaviour of Costa da Caparica Beaches Monitored during Nourishment Operations. *J. Coast. Res.* **2013**, *65*, 1862–1867. [[CrossRef](#)]
11. Silva, S.F.; Martinho, M.; Capitão, R.; Reis, T.; Fortes, C.J.; Ferreira, J.C. An index based method for coastal-flood risk assessment in low-lying areas (Costa de Caparica, Portugal). *Ocean. Coast. Manag.* **2017**, *144*, 90–104. [[CrossRef](#)]
12. Santos, Â.; Mendes, S.; Corte-Real, J. Impacts of the storm Hercules in Portugal. *Finisterra* **2014**, *XLIX* 98, 197–220. [[CrossRef](#)]
13. Brown, J.M.; Phelps, J.J.C.; Barkwith, A.; Hurst, M.-D.; Ellis, M.A.; Plater, A.J. The effectiveness of beach mega-nourishment, assessed over three management epochs. *J. Environ. Manag.* **2016**, *184*, 400–408. [[CrossRef](#)]
14. Stripling, S.; Panzeri, M.; Blanco, B.; Rossington, K.; Sayers, P.; Borthwick, A. Regional-scale probabilistic shoreline evolution modelling for flood-risk assessment. *Coast. Eng.* **2017**, *121*, 129–144. [[CrossRef](#)]
15. Pereira, C.; Coelho, C. Mapping erosion risk under different scenarios of climate change for Aveiro coast, Portugal. *Nat. Hazards* **2013**, *69*, 1033–1050. [[CrossRef](#)]
16. Chataigner, T.; Yates, M.L.; Le Dantec, N.; Harley, M.D.; Splinter, K.D.; Goutal, N. Sensitivity of a one-line longshore shoreline change model to the mean wave direction. *Coast. Eng.* **2022**, *172*, 104025. [[CrossRef](#)]
17. Fortunato, A.B.; Freire, P.; Mengual, B.; Bertin, X.; Pinto, C.; Martins, K.; Guérin, T.; Azevedo, A. Sediment dynamics and morphological evolution in the Tagus Estuary inlet. *Mar. Geol.* **2021**, *440*, 106590. [[CrossRef](#)]
18. Lira, C.P.; Nobre-Silva, A.; Taborda, R.; Andrade, C.F. Coastline evolution of Portuguese low-lying sandy coast in the last 50 years: An integrated approach. *Earth Syst. Sci. Data* **2016**, *8*, 265–278. [[CrossRef](#)]
19. Pinto, C.A.; Gomes, E.; Rodrigues, A. Dredging and beach nourishment: A sustainable sediment management approach in Costa da Caparica beach (Portugal). In Proceedings of the Dredging 2015 Conference Moving and Managing Sediments, Savannah, GA, USA, 19–22 October 2015.
20. Freire, P.; Fortunato, A.; Oliveira, F.S.B.F. *Modelação Para Apoio às Intervenções nas Praias da Costa da Caparica–Almada. Estudo IV–Avaliação do Comportamento e Longevidade das Alimentações Artificiais. Efeito do Forçamento*; Report 223/2019–DHA/NEC; LNEC: Lisbon, Portugal, 2019. (In Portuguese)
21. Veloso-Gomes, F.; Taveira-Pinto, F.; Pais-Barbosa, J. Rehabilitation study of coastal defense works and artificial sand nourishment at Costa da Caparica, Portugal. In Proceedings of the 29th International Conference of Coastal Engineering 2004, Lisboa, Portugal, 19–24 September 2004; pp. 3429–3440.
22. Raposo, P.D.; Fortes, C.J.E.M.; Capitão, R.; Reis, M.T.; Ferreira, J.C.; Pereira, M.T.S.; Guerreiro, J. Preliminary phases of the HIDRALERTA system: Assessment of the flood levels at S. João da Caparica beach, Portugal. In Proceedings of the 12th International Coastal Symposium 2013, Plymouth, UK, 9–12 April 2013; pp. 808–813. [[CrossRef](#)]
23. Garzon, J.L.; Ferreira, A.M.M.; Ferreira, Ó.; Fortes, C.J.; Reis, M.T. Beach State Report: Quarteira, Praia de Faro and Costa da Caparica. EW-Coast Project-Early Warning System for Coastal Risks Induced by Storms. 2020. ALG-LISBOA-01-145-FEDER-028657. Available online: <https://www.cima.ualg.pt/EW-COAST/> (accessed on 16 April 2023).
24. Sancho, F.; Silva, J.; Neves, M.G. Avaliação e quantificação da intensidade da agitação marítima no arco Caparica-Espichel. In Proceedings of the 9as Jornadas Portuguesas de Engenharia Costeira e Portuária 2017, Lisboa, Portugal, 23–24 November 2017.
25. Dodet, G. Morphodynamic Modelling of a Wave-Dominated Tidal Inlet: The Albufeira Lagoon. Ph.D. Thesis, La Rochelle University, École Doctorale Sciences pour L’Environnement Gay-Lussac, La Rochelle, France, 2013; 181p.
26. Fortunato, A.B.; Baptista, A.M.; Luettich, R.L., Jr. A three-dimensional model of tidal currents in the mouth of the Tagus estuary. *Cont. Shelf Res.* **1997**, *17*, 1689–1714. [[CrossRef](#)]
27. Taborda, R.; Andrade, C. Morfodinâmica do Estuário Exterior do Tejo e Intervenção na Região da Caparica–v1. In *Report Contributo para o Grupo de Trabalho do Litoral*; Lisbon, Portugal, 2014. (In Portuguese)
28. Sancho, F. *Modelação Para Apoio às Intervenções Nas Praias da Costa da Caparica–Almada; Estudo II–Modelação da Evolução Morfológica para Diferentes Cenários de Intervenção. Aplicação do Modelo*; Report 111/2020–DHA/NEC; LNEC: Lisbon, Portugal, 2020. (In Portuguese)

29. Diogo, Z.S.; Silveira, T.M.; Sousa, H.; Carapuço, A.M.; Silva, A.N.; Taborda, R.; Andrade, C. *Estudo de Caso da Costa da Caparica; Caracterização da Variabilidade Morfodinâmica Sazonal e Pós-Temporal das Praias da Costa da Caparica–Entregável 2.2.c*; FCUL: Lisbon, Portugal, 2013; 119p. (In Portuguese)
30. Freire, M.E.F. A planície litoral entre Trafaria e a Lagoa de Albufeira-estudo de geomorfologia litoral. *Estudos (SNPRCN)* **1989**, *3*, 1–204.
31. Hallermeier, R. Uses for a calculated limit depth to beach erosion. In *Coastal Engineering Proceedings*; ASCE: Hamburg, Germany, 1978; Volume 1, p. 88. [CrossRef]
32. Programa COSMO. Available online: <https://cosmo.apambiente.pt> (accessed on 20 March 2023).
33. Boak, E.H.; Turner, I.L. Shoreline definition and detection: A review. *J. Coast. Res.* **2005**, *21*, 688–703. Available online: <http://www.jstor.org/stable/4299462> (accessed on 30 March 2023). [CrossRef]
34. Buccino, M.; Di Paola, G.; Ciccaglione, M.C.; Del Giudice, G.; Roskopf, C.M. A Medium-Term Study of Molise Coast Evolution Based on the One-Line Equation and “Equivalent Wave” Concept. *Water* **2020**, *12*, 2831. [CrossRef]
35. Silva, A.N.; Lira, C.; Matildes, R.; Andrade, C.; Taborda, R.; Freitas, M.C. *Utilização de Ortofotomapas e Fotografias Aéreas Para a Delimitação da Linha de Costa–Entregável 1.2.2.2.c*; FCUL: Lisbon, Portugal, 2013; 59p. (In Portuguese)
36. Hapke, C.J.; Himmelstoss, E.A.; Kratzmann, M.; List, J.H.; Thieler, E.R. *National Assessment 528 of Shoreline Change: Historical Shoreline Change Along the New England and Mid-Atlantic 529 Coasts. Open-File Report 2010-1118*; U.S. Geological Survey: Reston, VA, USA, 2010; p. 57.
37. Booij, N.; Ris, R.C.; Holthuijsen, L.H. A third-generation wave model for coastal regions, Part I, Model description and validation. *J. Geophys. Res.* **1999**, *104*, 7649–7666. [CrossRef]
38. Dodet, G.; Bertin, X.; Taborda, R. Wave climate variability in the North-East Atlantic Ocean over the last six decades. *Ocean. Model.* **2010**, *31*, 120–131. [CrossRef]
39. Rusu, L.; Bernardino, M.; Guedes-Soares, C. Wave forecast at the entrance of the Tagus estuary. In *Proceedings on the Third International Conference on the Application of Physical Modelling to Port and Coastal Protection, COASTLAB-2010*; Black Sea Coastal Research Association: Varna, Bulgaria, 2014.
40. Fortunato, A.B.; Nahon, A.; Dodet, G.; Pires, A.R.; Freitas, M.C.; Bruneau, N.; Azevedo, A.; Bertin, X.; Benevides, P.; Andrade, C.; et al. Morphological evolution of an ephemeral tidal inlet from opening to closure: The Albufeira inlet, Portugal. *Cont. Shelf Res.* **2014**, *73*, 49–63. [CrossRef]
41. Vicente, C.; Clímaco, M. *Evolução de Linhas de Costa. Desenvolvimento e Aplicação de um Modelo Numérico*; Report ICT-ITH 42; LNEC: Lisbon, Portugal, 2003. (In Portuguese)
42. Oliveira, F.S.B.F.; Freire, P.; Sancho, F.; Vicente, C.M.; Clímaco, C. Rehabilitation and protection of Colwyn Bay beach: A case study. In *Proceedings of the 11th International Coastal Symposium 2013, Szczecin, Poland, 9–13 May 2011*; pp. 1272–1276.
43. Hanson, H. Genesis: ‘A generalized shoreline change numerical model’. *J. Coast. Res.* **1989**, *5*, 1–27.
44. Kamphuis, J.W. Alongshore Sediment Transport Rate. *J. Waterw. Coast. Ports Ocean. Eng.* **1991**, *11*, 624–640. [CrossRef]
45. Dean, R.G. *Equilibrium Beach Profiles: U.S. Atlantic and Gulf Coasts*; Ocean Engineering Technical Report No. 12; Department of Civil Engineering and College of Marine Studies, University of Delaware: Newark, DE, USA, 1977.
46. Duarte-Santos, F.; Mota-Lopes, A.; Moniz, G.; Ramos, L.; Taborda, R. *Grupo de Trabalho do Litoral: Gestão da zona Costeira. O desafio da Mudança*; Duarte Santos, F., Penha-Lopes, G., Mota Lopes, A., Eds.; Agência Portuguesa do Ambiente: Lisboa, Portugal, 2018; 368p, ISBN 978-989-99962-1-2. (In Portuguese)
47. Mota-Oliveira, I.B. Port of Lisbon improvement of the access conditions through the Tagus estuary entrance. *Coast. Eng. Proc.* **1992**, *1*, 2745–2757. [CrossRef]
48. Silva, A.N.; Lira, C.; Sousa, H.; Silveira, T.M.; Andrade, C.; Taborda, R.; Freitas, M.C. Análise da Evolução da Linha de Costa nos Últimos 50 Anos–Caso Especial da Costa da Caparica–Entregável 1.2.2.2.b. FCUL: Lisbon, Portugal, 2013; 24p. (In Portuguese)
49. Canelas, S.T.; Sancho, F.; Trigo-Teixeira, A. A Coastal Defense Work Plan 40 Years Later: Review and Evaluation of the Espinho Case Study in Portugal. *J. Waterw. Port Coast. Ocean. Eng.* **2022**, *148*, 05022004. [CrossRef]
50. Hanson, H.; Larson, M.; Kraus, N.C. A new approach to represent tidal currents and bathymetric features in the oneline model concept. *Proc. Coast. Dyn.* **2001**, *1*, 172–181.
51. Hanson, H.; Kraus, N.C. *GENESIS-Generalized Model for Simulating Shoreline Change. Vol. 1: Reference; Manual and Users Guide Technical Report CERC-89-19*; Coastal Engineering Research Center, U.S. Army Corps of Engineers: Washington, DC, USA, 1989; 247p.
52. Antolínez, J.A.A.; Méndez, F.J.; Anderson, D.; Ruggiero, P.; Kaminsky, G.M. Predicting climate-driven coastlines with a simple and efficient multiscale model. *J. Geoph. Res. Earth Surf.* **2019**, *124*, 1596–1624. [CrossRef]
53. Mil-Homens, J.; Ranasinghe, R.; van Thiel de Vries, J.S.M.; Stive, M.J.F. Re-evaluation and improvement of three commonly used bulk longshore sediment transport formulas. *Coast. Eng.* **2013**, *75*, 29–39. [CrossRef]
54. Pilkey, O.; Cooper, A. Longshore transport volumes: A critical view. *J. Coast. Res.* **2002**, *36*, 572–580. [CrossRef]
55. Barceló, J.P. *Esporões Marítimos–Funcionamento Hidráulico de Unidades Fisiograficamente Independentes*; LNEC: Lisboa, Portugal, 1966; 115p. (In Portuguese)
56. TECHINT. *Estudo do Aproveitamento Turístico da Área da Cova do Vapor*; Compagnia Tecnica Internazionale: Castellanza, Italy, 1966. (In Portuguese)
57. Taborda, R.; Andrade, F.C.; Silva, N.A.; Silveira, M.T.; Lira, C.; Freitas, C.M.; Pinto, C. Caparica-Espichel Longshore Sediment Transport Model. In *Proceedings of the IX Congresso Nacional de Geologia, Comunicações Geológicas, Porto, Portugal, 18–24*

- July 2014; Volume 101, pp. 641–644. Available online: <http://www.lneg.pt/iedt/unidades/16/paginas/26/30/185> (accessed on 30 March 2023). (In Portuguese).
58. Pinto, C.; Silveira, T.; Teixeira, S. *Alimentação Artificial de Praias na Faixa Costeira de Portugal Continental: Enquadramento e Retrospectiva das Intervenções Realizadas (1950–2017)*; Relatório técnico; Departamento do Litoral e Proteção Costeira. Núcleo de Monitorização Costeira e Risco: Amadora, Portugal, 2018; 61p. (In Portuguese)
59. Pais, D.; Andrade, C.; Pinto, C. Evolution of a beach-dune system after artificial nourishment: The case of São João da Caparica (Portugal). In Proceedings of the Building Coastal Resilience 2022, Dune in Front of a Dike International Conference, KU Leuven Bruges Campus, Bruges, Belgium, 12–13 April 2022.

Disclaimer/Publisher’s Note: The statements, opinions and data contained in all publications are solely those of the individual author(s) and contributor(s) and not of MDPI and/or the editor(s). MDPI and/or the editor(s) disclaim responsibility for any injury to people or property resulting from any ideas, methods, instructions or products referred to in the content.